JOURNAL OF GUIDANCE, CONTROL, AND DYNAMICS
Vol. 21, No. 4, July–August 1998

Digitally Redesigned Pulse-Width Modulation Spacecraft Control

Douglas J. Zimpfer*
Charles Stark Draper Laboratory, Inc., Houston, Texas 77058
Leang S. Shieh†
University of Houston, Houston, Texas 77204
and
John W. Sunkel‡
NASA Johnson Space Center, Houston, Texas 77058

A new method is presented for the design of control laws for systems with on–off nonlinear actuators. The new methodology improves the design of control laws for pulse-modulated systems by allowing the use of continuous-time, multi-input/multi-output design procedures. Discrete-time state feedback control gains are developed from the digital redesign of continuous-time feedback gains, based on a geometric series approximation, to closely match the states of the closed-loop hybrid system to those of the original designed closed-loop, continuous-time system at each sampling instant. A delay is then incorporated into a pulse-width modulator design to closely match the states of the modulated system to those of the discrete-time, pulse-amplitude modulated system. The delay time is improved from previous work to provide a close match between the states for pulse durations of all sizes, in effect matching the states of the pulse-width modulated system to those of the closed-loop, continuous-time system. The new control law design is applied to the problem of attitude control of the Space Shuttle Orbiter with the Hubble Space Telescope deployed on its remote manipulator.

Introduction

MANY paradigms are available for the synthesis of control laws for continuous-time systems, and though many methods also exist for developing discrete-time or digital controllers, it is often desirable to design a control law for the continuous-time plant. It is often more direct to determine the control specifications in the continuous-time or frequency domain. Also, direct digital control law design has difficulty in predetermining the hybrid control specifications and ignores intersampling effects. Nevertheless, these continuous-time control laws are generally implemented via discrete-time computer control, requiring that a discrete-time control, equivalent to the continuous-time control, be developed. The process of developing discrete-time control laws that provide closed-loop performance of the hybrid system equivalent to the performance of the designed closed-loop, continuous-time system is known as digital redesign. Several techniques have been developed to digitally redesign continuous-time feedback controllers.[1–3]

Unfortunately, the principal applied for the design of discrete-time control laws, i.e., that the amplitude of the control signal can take any finite value, which is why discrete-time control is often referred to as pulse-amplitude control (PAM), is not valid for all computer-controlled systems. Systems that utilize on–off control devices, such as the reaction jet or electronic relay, can only provide a single finite value of control. To provide control with these types of actuators, either complex nonlinear algorithms[4] must be developed or the control must be applied by modulating the pulse width, the pulse frequency, or both the pulse width and frequency. These modulation techniques, in particular pulse-width modulation (PWM), allow the design of linear control laws to control nonlinear systems. Although methods exist for the design of linear control laws for PWM systems,[5] they still rely heavily on using single-input/single-output plant models and nonlinear stability analysis techniques to determine pulse modulator parameters. Another method used in the design of PWM control laws, which provides a measure of stability but does not minimize the error between the discrete-time model and the PWM model, is to treat the error as a bounded uncertainty to be included in the design or stability analysis of the system.[6]

Recently, a method was proposed to include a delay in the application of the pulse to minimize the error between the PWM and PAM models.[7] The delay is developed on the assumption that the pulse duration will always be small compared to the sample time of the discrete-time control. For systems meeting this assumption, stability of the closed-loop, discrete-time system is maintained, that is, multi-input/multi-output control can be applied and the steady-state error between the PWM and PAM systems is minimized.

This work extends the previous efforts by applying improved methods for both the digital redesign of the continuous-time, state feedback gains and the calculation of an appropriate delay in the application of the pulsed control input. Additionally, the two techniques are combined to develop a pulse modulated control law that closely matches the states of the closed-loop, hybrid (discrete control law, pulse modulated control, and continuous-time plant) system to those of the original closed-loop, continuous-time system. The digital redesign of the state feedback gains is based on a second-order geometric series approximation[8] of the discrete-time system, whereas the pulse delay is calculated based on the system itself and the pulse duration.

The new design method is applied to the problem of attitude control for the Space Shuttle Orbiter with the Hubble Space Telescope deployed on its robotic arm to demonstrate the performance of the proposed design technique.

Linear Control Law Design

The first step in the design of the control law is to determine a continuous-time, state feedback control that meets the required performance specifications. Although several regulator design techniques exist to determine the state feedback gains, placement of the closed poles in a vertical strip[9] is employed here. Next the continuous-time gains are digitally redesigned to provide discrete-time gains. These discrete-time gains provide equivalent closed-loop performance by closely matching the states of the hybrid system to the continuous-time, closed-loop system at each sampling instant.

Received Sept. 26, 1994; presented as Paper 95-3361 at the AIAA Guidance, Navigation, and Control Conference, Baltimore, MD, Aug. 7–10, 1995; revision received March 23, 1998; accepted for publication March 24, 1998.

*Senior Member Technical Staff, Control and Dynamical Systems. Member AIAA.
†Professor, Electrical Engineering. Member AIAA.
‡Aerospace Engineer, Flight Mechanics and Aerosciences Division. Member AIAA.

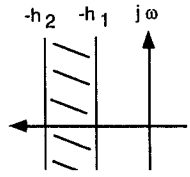

Fig. 1 Pole placement in a vertical strip.

State Feedback

Given the continuous-time, state-space system

$$\dot{X}(t) = AX(t) + Bu(t), \qquad y(t) = CX(t) \tag{1}$$

the standard linear quadratic regulator theory minimizes the cost function

$$J = \frac{1}{2}\int_{t_0}^{\infty} [X(t)^T QX(t) + u(t)^T Ru(t)]\,dt$$

$$Q \geq 0, \qquad R > 0 \tag{2}$$

by solving the algebraic Riccati equation (ARE)

$$PA + A^T P + Q - PBR^{-1}B^T P = 0 \tag{3}$$

to determine state-feedback control gains

$$K = R^{-1}B^T P \tag{4}$$

where Q and R are used as weighting functions. Direct control over the placement of the closed-loop poles can be obtained by modifying the cost function in Eq. (2) to place the poles in a vertical strip, as shown in Fig. 1. This results in minimizing the cost function

$$J = \frac{1}{2}\int_0^{\infty} e^{2\alpha t}[X(t)^T QX(t) + u(t)^T Ru(t)]\,dt \tag{5}$$

by solving the ARE

$$\hat{A}P + \hat{A}^T P - PBR^{-1}B^T P = 0 \tag{6}$$

where

$$\hat{A} = A + \alpha I_n \tag{7}$$

and the feedback gains are determined from

$$K = \gamma R^{-1}B^T P \tag{8}$$

where

$$\gamma = \frac{1}{2} + \frac{h_2 - h_1}{\text{tr}(BR^{-1}B^T P)} \tag{9}$$

If

$$h_2 > \max(\text{Re}(|\lambda(A)|)) \tag{10}$$

then all of the closed-loop poles lie in the vertical strip of Fig. 1. It should be noted that stable poles to the left of the vertical strip may not migrate to within the strip.

Geometric Series Digital Redesign

To implement the state-feedback control into a digital computer, the continuous-time gains calculated in Eq. (4) or Eq. (8) must be digitally redesigned to provide discrete-time gains that provide equivalent system performance, i.e., the states of the closed-loop hybrid system closely match the states of the closed-loop, continuous-time system at each sampling instant. Geometric series modeling of discrete-time systems is applied to develop discrete-time gains that closely match the states, even for relatively long sampling periods near the Nyquist period.

To develop the discrete-time model

$$X(k+1) = GX(k) + Hu(k), \qquad y = CX(k) \tag{11}$$

equivalent to the continuous-time model of Eq. (1), Shieh et al.[8] proposed a geometric series approximation of the Taylor series expansion of e^{AT}:

$$G = e^{AT}$$

$$= I_n + AT + \frac{(AT)^2}{2!} + \frac{(AT)^3}{3!} + \frac{(AT)^4}{4!} + \cdots \tag{12}$$

by

$$G = \left[e^{-\frac{1}{2}AT}\right]^{-1}\left[e^{\frac{1}{2}AT}\right] \cong Q_j^{-1}P_j \triangleq G_j \tag{13}$$

where

$$Q_j = \left[I_n - \frac{1}{2j}AT\right]\left[I_n + \sum_{i=1}^{j-1}\frac{(-1)^i(j-i)}{(2^i)(j)(i!)}(AT)^i\right]$$

$$P_j = \left[I_n + \frac{1}{2j}AT\right]\left[I_n + \sum_{i=1}^{j-1}\frac{(j-i)}{(2^i)(j)(i!)}(AT)^i\right]$$

$$T < \frac{2j}{\|A\|} \qquad \text{for} \qquad j = 1, 2, \ldots$$

resulting in a second-order approximation of

$$G_2 = \left[I_n - \tfrac{1}{2}AT + \tfrac{1}{16}(AT)^2\right]^{-1}\left[I_n + \tfrac{1}{2}AT + \tfrac{1}{16}(AT)^2\right]$$

$$\approx G \tag{14}$$

and

$$H_2 = \left[I_n - \tfrac{1}{2}AT + \tfrac{1}{16}(AT)^2\right]^{-1}BT \approx H \tag{15}$$

This geometric series is applied to determine discrete-time feedback gains that match the states of the closed-loop, continuous-time system to those of the closed-loop, discrete-time system at each sampling instant $X_{cd}(kT) = X_c(t)|_{t=KT}$, where $X_{cd}(kT)$ and $X_c(t)$ are the states of the closed-loop, discrete-time and continuous-time systems, respectively. The objective of digital redesign is to find the discrete-time feedback gain K_d that matches the states of the closed-loop systems at each sampling instant. Let, $\hat{G} = e^{(A-BK_c)T}$, where K_c is the continuous-time, state feedback gain, then find the discrete-time control gain K_d that satisfies

$$\hat{G} = G - HK_d \tag{16}$$

at each sampling instant kT.

Applying a geometric series to approximate $\hat{G}$ provides

$$\hat{G} = e^{\hat{A}T} = e^{(A+\Delta A)T} \approx \hat{G}_2, \qquad \hat{G}_2 = [I_n - \Delta P]^{-1}[I_n + \Delta P] \tag{17}$$

where

$$\Delta P = \tfrac{1}{2}(A + \Delta A)T + \tfrac{1}{16}(A + \Delta A)^2T^2$$

and $\Delta A = -BK_c$ and $\hat{A} = A - BK_c$, and K_c is the continuous-time, state feedback gain. This can be rewritten as

$$\hat{G} \approx \hat{G}_2 = G + \left[I_n - \tfrac{1}{2}\hat{A}T + \tfrac{1}{16}(\hat{A}T)^2\right]^{-1}$$

$$\times \left[\tfrac{1}{2}\Delta A(G + I_n)T + \tfrac{1}{16}[A\Delta A + \Delta AA + \Delta AA^2](G - I_n)T^2\right] \tag{18}$$

or

$$\hat{G} \approx G + \Delta G \tag{19}$$

where

$$\Delta G = \left[I_n - \tfrac{1}{2}\hat{A}T + \tfrac{1}{16}(\hat{A}T)^2\right]^{-1}$$

$$\times \left[\tfrac{1}{2}\Delta A(G + I_n)T + \tfrac{1}{16}[A\Delta A + \Delta AA + \Delta AA^2](G - I_n)T^2\right] \tag{20}$$

Setting ΔG equal to $-HK_d$, we can explicitly solve for the desired values of K_d to match the states of the discrete-time system to those of the continuous-time system. Applying the pseudoinverse of ΔA and the matrix inverse lemma gives

$$\Delta G = -\tfrac{1}{2}HPK_c(G + I_n) + (T/16)HPK_c(\bar{A} + \hat{A})(G - I_n) \tag{21}$$

providing

$$K_d = \tfrac{1}{2} P K_c[(G + I_n) - (T/8)(\bar{A} + \hat{A})(G - I_n)] \tag{22}$$

where

$$P = \left\{ I_m + \tfrac{1}{2} K_c \left[I_n - \tfrac{1}{8}(\bar{A} + \hat{A})T \right] H \right\}^{-1}$$

and $\hat{A} = A + \Delta A = A - BK_c$ and $\bar{A} \triangleq (\Delta A)^+ A \Delta A \in \Re^{n \times n}$, with $(\Delta A)^+ \in \Re^{n \times n}$ the pseudoinverse of ΔA.

Given the continuous-time, feed forward gain E_c, the discrete-time, feed forward gain E_d is obtained in a similar manner from

$$\hat{H} E_c = [G - I_n]\hat{A}^{-1} B E_c \approx \hat{H}_2 E_c \tag{23}$$

and

$$\hat{H}_2 E_c \approx H \left\{ I_m + \tfrac{1}{2} K_c [I_n - (T/8)(\bar{A} + \hat{A})] H \right\}^{-1} E_c \tag{24}$$

providing

$$E_d = \left\{ I_m + \tfrac{1}{2} K_c [I_n - (T/8)(\bar{A} + \hat{A})] H \right\}^{-1} E_c \tag{25}$$

Therefore, the discrete-time, state feedback gain K_d along with the feed forward gain E_d can be applied at each sample time kT to match the states of the closed-loop hybrid system to those of the original closed-loop, continuous-time system.

PWM Design

For systems with a constant magnitude on–off control, such as reaction jets and/or electronic relays, the amplitude of the control cannot be modulated. Therefore, the duration or width of the control signal must be modulated. Figure 2 provides a graphical comparison of the PAM and PWM systems. Typically, the duration of the pulse width is computed based on the principal of equivalent area[10] and placed at the beginning of the sample period ($\tau = 0$). The method employed here will also utilize the principal of equivalent area, but the pulse will be delayed to minimize the error between the PAM and PWM states.

The response of the system to discrete-time control inputs u_d is

$$x(t + T) = e^{AT} + \left(\sum_{i=0}^{\infty} \frac{A^i}{(i+1)!} T^i \right) B T u_d \tag{26}$$

whereas the response of the system to a pulse modulated control, with a pulse duration of δ, pulse delay of τ, and a constant control magnitude of u_M, is given by

$$x(t + T) = e^{AT} + e^{A(T-\tau)} \left(\sum_{i=0}^{\infty} \frac{A^i}{(i+1)!} (-\delta)^i \right) B \delta u_M \tag{27}$$

resulting in an error between the states of PAM and PWM systems,

$$e = \left(\sum_{i=0}^{\infty} \frac{A^i}{(i+1)!} T^i \right) B T u_d - e^{A(T-\tau)} \left(\sum_{i=0}^{\infty} \frac{A^i}{(i+1)!} (-\delta)^i \right) B \delta u_M \tag{28}$$

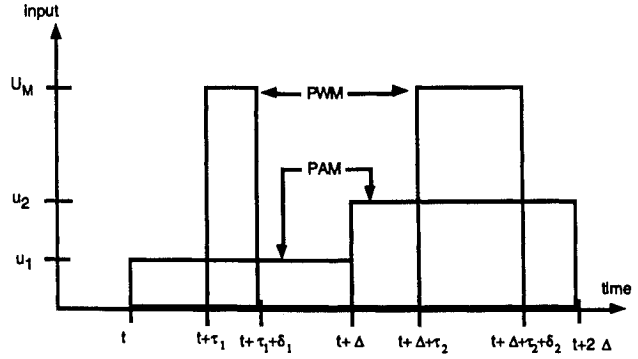

Fig. 2 Graphical representation of discrete and PWM controls.

Applying the principal of equivalent area, the pulse width is calculated as

$$u_d T = u_M \delta, \qquad \delta = u_d T / u_M \tag{29}$$

Bernelli-Zazzera and Mantegazza[7] applied calculus of variations[11] to approximate a delay to minimize the error between the PAM and PWM systems for short-duration pulses, i.e., pulse durations that allowed for a first-order approximation of

$$e^{-A\delta} = I - A\delta \tag{30}$$

resulting in a delay time

$$\bar{\tau} = \frac{T}{2} - \Delta\tau = \frac{T}{2} - \frac{B^t(\Xi - \Theta)^t(\Xi - \Theta)B}{B^t[\Theta^t A^t(\Xi - \Theta) + (\Xi - \Theta)^t A \Theta]B} \tag{31}$$

where

$$\Theta = e^{AT/2} \tag{32}$$

and

$$\Xi = \sum_{i=0}^{\infty} \frac{A^i}{(i+1)!} T^i \tag{33}$$

Although this provides a close match between the states of the PAM and PWM systems for the steady-state response of systems with a large-amplitude control u_M, resulting in small pulse durations, it does not work well for the transient response and for systems that operate with smaller control signals, requiring longer pulse durations.[12]

Recognizing that the delay in Eq. (31) provides a close match of the system states when the pulse duration is small, it is clear that for longer pulse durations the pulse should be centered around this delay time. A weighting function, geometrically shown in Fig. 3, can be applied to determine a new delay time

$$\hat{\tau} = \bar{\tau} - W\delta \tag{34}$$

where W is a function of the pulse duration and determines the portion of the pulse to be applied prior to the optimal delay for short pulses. Because the weighting function is determined a priori as a function of the pulse duration, complex functions could be determined to optimize varying performance criteria. To simplify the effort here, a constant-value W is obtained by recognizing that as the pulse duration approaches the sample time T the delay time $\hat{\tau}$ should approach 0. Solving this boundary condition provides the weighting function

$$\hat{\tau} = 0 = \bar{\tau} - WT \Rightarrow W = \bar{\tau}/T \tag{35}$$

The other boundary condition, that as the pulse duration approaches zero the delay time should approach $\bar{\tau}$, is achieved in the limit by the duration itself approaching zero. To meet both boundary conditions simultaneously, a second degree of freedom must be added by increasing the complexity of the weighting function.

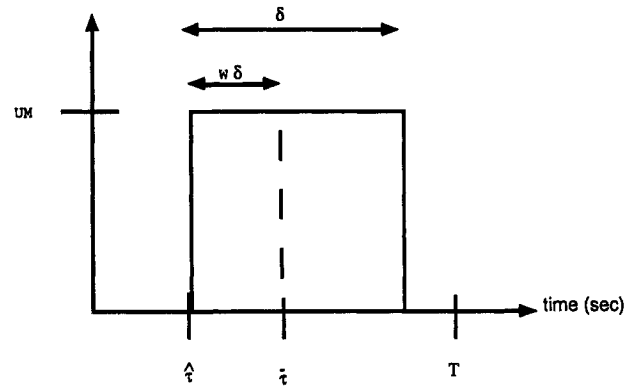

Fig. 3 Geometric pulse delay weighting function.

Example: Space Shuttle Attitude Control

To demonstrate the proposed design methodology, an attitude control law was developed for the Space Shuttle. The design plant consisted of the rigid-body dynamics of the Space Shuttle with the Hubble Space Telescope (HST) deployed on the remote manipulator system (RMS) and the flexible dynamics of the HST extended on the RMS were treated as an additive uncertainty. The plant was a linearized model of the Shuttle jet selection and plant dynamics, with rotational commands as inputs and rate and attitude states as measurement outputs. The pulse modulator acts to determine pulse durations or firing times for the rotational commands distributed to the jet selection logic, which determines the appropriate set of jets to achieve the desired command. A table-lookup selection scheme was employed to meet the constant control assumption of the pulse modulated system. The derivation of the linear plant is provided in Ref. 12.

The Shuttle/RMS/HST plant model consisted of the three rigid-body modes and six flex-body modes with frequencies [0.2946, 0.3420, 0.5063, 0.7539, 1.2799, 2.1405] rad/s, and 2% damping.

First, a continuous-time, state-feedback control law was developed for the rigid-body plant to place the poles in the vertical strip defined by {0.025, 0.028}, to meet the control specifications in Table 1. This resulted in

$$K_c =$$

$$\begin{bmatrix} 0.1590 & -0.0120 & 0.0123 & 6.4227 & -0.4852 & 0.4967 \\ -0.0015 & 0.1144 & 0.0025 & -0.0597 & 4.6243 & 0.1015 \\ 0.0164 & 0.0030 & 0.1710 & 0.6623 & 0.1207 & 6.9098 \end{bmatrix} \tag{36}$$

Figure 4 provides the singular value response of the designed continuous-time control law for the design plant and the actual plant with additive uncertainty, indicating the control provides acceptable attenuation of the flex-body dynamics.

Table 1 Control design specifications

Specification	Criterion
Rise time	$\leq$100 s
Damping	$\zeta > 0.7$
Control energy	$\lvert u \rvert \leq 1$
Disturbance rejection	Stable to uncertainty
Attitude error	$\leq$0.1 deg

Next, the geometric series digital redesign technique was applied to determine the discrete-time control gains for a sample time $T = 5$ s, as

$$K_d =$$

$$\begin{bmatrix} 0.1398 & -0.0106 & 0.0108 & 6.0103 & -0.4540 & 0.4648 \\ -0.0013 & 0.1007 & 0.0022 & -0.0558 & 4.3273 & 0.0950 \\ 0.0144 & 0.0026 & 0.1504 & 0.6197 & 0.1129 & 6.4661 \end{bmatrix} \tag{37}$$

The pulse modulation parameters were determined based on the flexible dynamics of the system. The pulse delay was determined

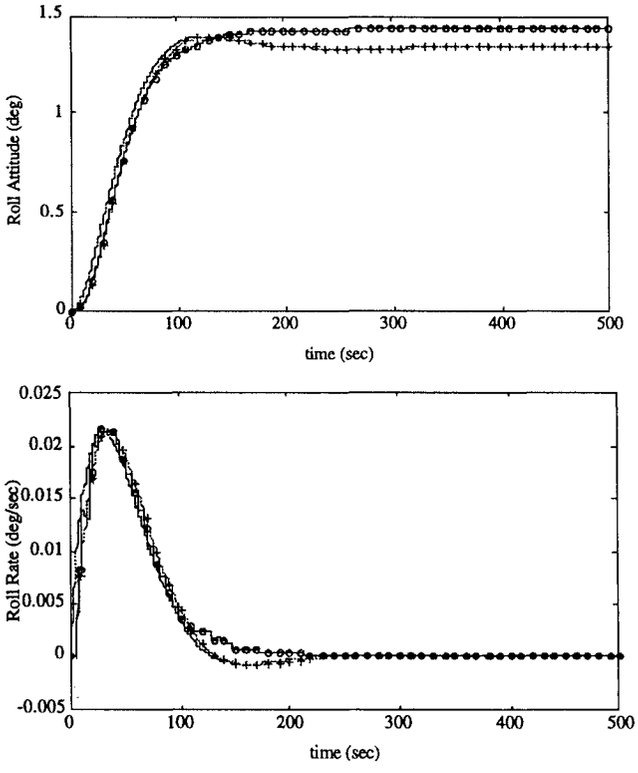

Fig. 5 Roll axis response comparison, rigid-body design plant: +, discrete; ○, PWM; and no symbol, continuous.

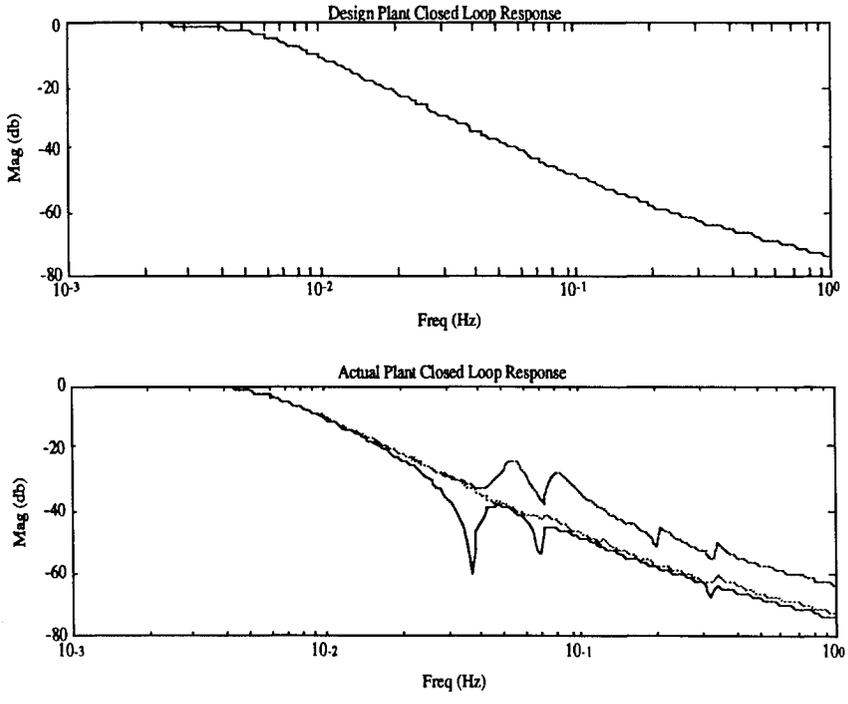

Fig. 4 Closed-loop frequency response.

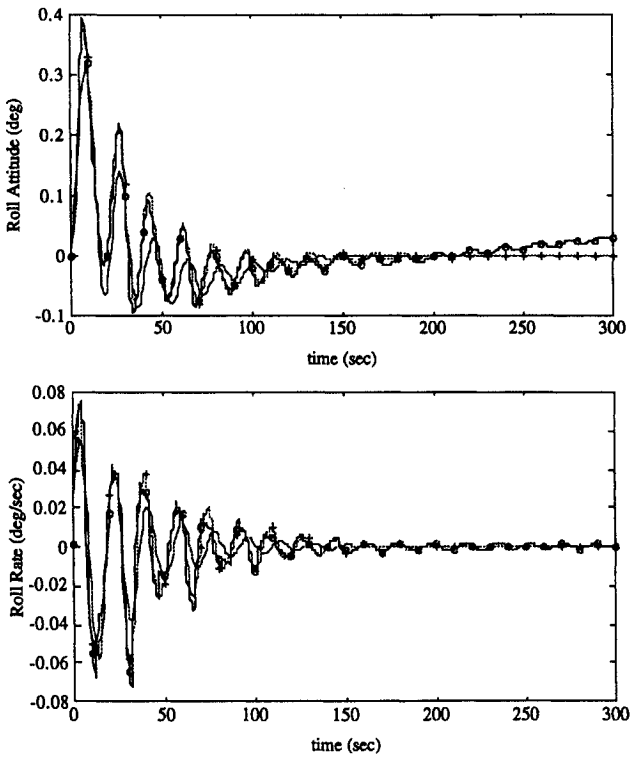

Fig. 6 Roll axis system response comparison, actual flexible plant: +, discrete; o, PWM; and no symbol, continuous.

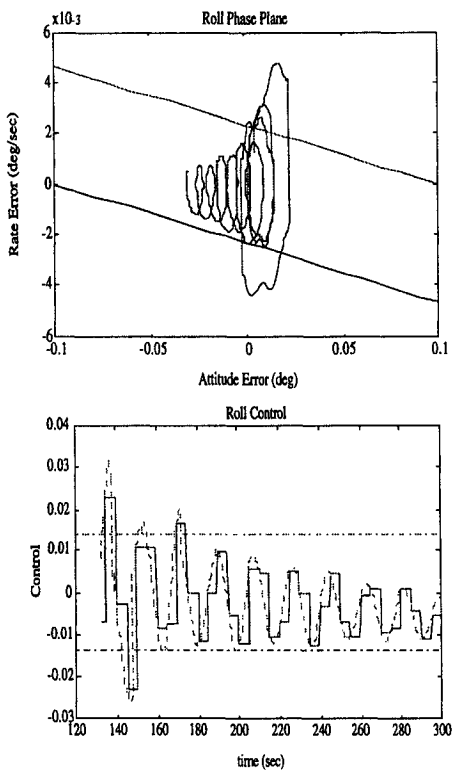

Fig. 7 PWM roll axis limit cycle response, actual flexible plant.

to be $\hat{\tau} = \bar{\tau} - W\delta$, where $\bar{\tau} = 2.9$ s and $W = 0.58$. To eliminate chattering of the pulse modulated controlled states about the steady-state reference, a deadband was employed to the control signal. The parameters of the deadband nonlinearity were selected to achieve acceptable limit cycle characteristics.

Figure 5 compares the roll axis attitude and rate response of the continuous-time, discrete-time, and PWM-controlled systems for the rigid-body design plant. The responses of the three systems match quite well, although the unique feature of the PWM system can be seen as a deadband was employed to eliminate control chattering around the steady-state value, resulting in acceptably small error in the vehicle attitude. Without this deadband, the error between the systems would be further minimized, but high-frequency chattering about the steady-state rate value would be incurred. The deadband was applied to the control signal based on acceptable attitude and rate error tolerances at steady state.

Figure 6 compares the performance for the actual plant model with the additive uncertainty included. The roll axis attitude and rate states are shown in response to a significant excitation in the lowest frequency flex mode, which is a roll mode. The state feedback gains developed for the rigid-body design plant were employed as output feedback on the measurement, which consisted of the combined rigid-body and flex-body states. Again the results of the three systems match quite well. The error between the continuous-time response and the discrete-time and PWM responses is induced from the slow 5-s sample rate, which is quite close to the periods of the middle frequencies of interest. As predicted from the continuous-time eigenvalues, the phase plane response of the actual plant to the control gains designed, as shown in Fig. 7, is stable, and the additive uncertainty does not induce unstable limit cycles in the nonlinear deadband.

For the Shuttle/HST/RMS model, the attitude controller is not required to explicitly control the motion of the payload via the Shuttle reaction jets. Therefore, a Kalman filter was employed based on the modeling uncertainty to estimate the rigid-body states from the combined system measurements corrupted by the additive uncertainty. Figure 8 compares the roll axis response with the Kalman

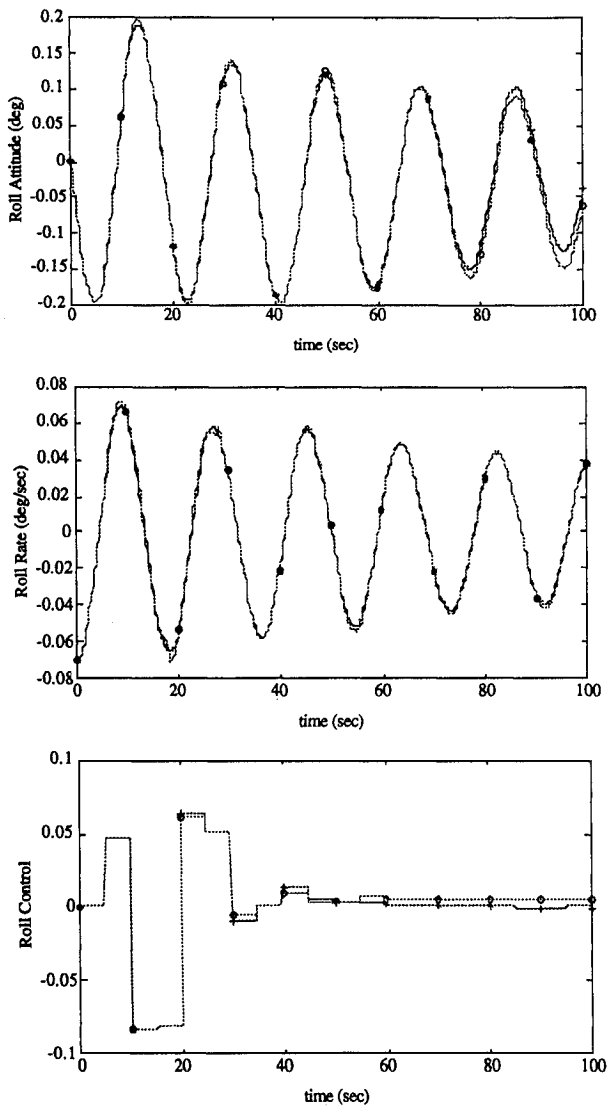

Fig. 8 Roll axis response with Kalman filter, actual flexible plant: +, discrete; o, PWM; and no symbol, continuous.

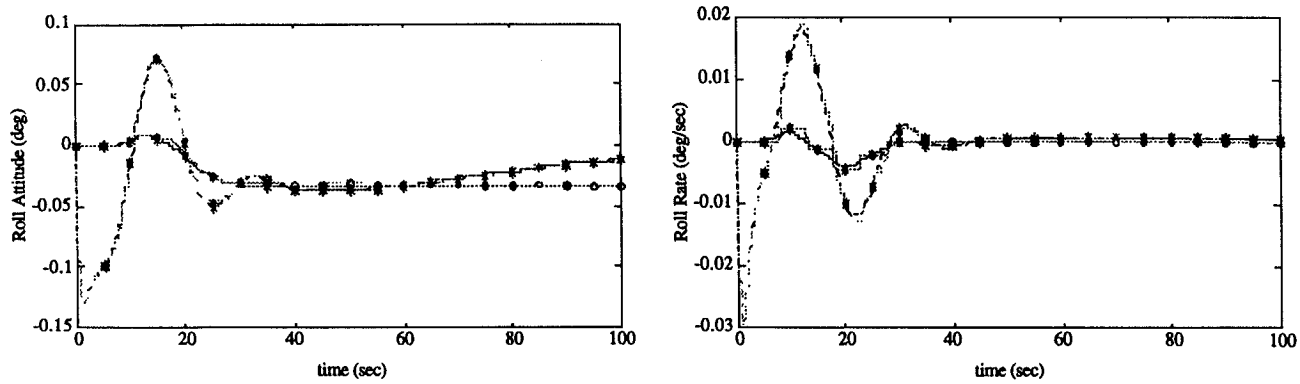

Fig. 9 Rigid-body attitude and rate estimates for PWM.

filter included for both the discrete-time and PWM-controlled systems. The response clearly indicates that little effort was employed by the controller to damp the modal oscillations, beyond the initial response to the filter transient. An excellent estimate of the rigid-body states was achieved as seen in Fig. 9, and the control effort expended to damp the oscillations seen in the preceding example was eliminated by the filter. The response in Fig. 9 indicates the Kalman filter designed for the discrete-time system also provided a good estimate for the PWM system. This was partially a result of the minimum pulse size of the control, selected to correspond to the sample time of the discrete filter. If the filter time were significantly larger than the minimal pulse duration, significant degradation in the filter performance would have been expected.

Conclusions

A design methodology has been presented to develop control laws for systems controlled by constant magnitude on–off control actuators. First, a continuous-time, linear, state-feedback control law is developed from a linear plant model to meet the required performance specifications. Next, the continuous-time, state-feedback gains are digitally redesigned via a geometric series method to find a discrete-time control law that closely matches the states of the discrete controlled system to the original closed-loop, continuous-time system at each sample instant. Finally, a PWM is developed, employing a delay in the pulse, to minimize the errors between the states of the discrete-time controlled system and the PWM-controlled system. Consequently, the PWM-controlled system response closely matches the original closed-loop, continuous-time response at each discrete sample instant.

Results were supplied demonstrating that the new design methodology provided an acceptable control law for attitude control of the Space Shuttle with the HST extended on the RMS. The design plant was based on the rigid-body dynamics of the system, and the flexible-body dynamics resulting from the HST extended on the RMS were treated as an additive uncertainty. The simulations indicated that for the rigid-body design plant the states of the PWM-controlled system closely matched the original continuous-time design. The deadband employed to avoid jet chattering around the steady-state value eliminated jet chattering, inducing acceptable attitude and rate errors within the specified limit cycle characteristics. When the additive uncertainty was included in the simulations, the match between the discrete-time and PWM-controlled systems and the continuous-time system was slightly degraded. This degradation resulted from attempting to control bending modes with periods only slightly longer than the control sample period. Although the performance was slightly degraded, an acceptable match between the system response was obtained. Additionally, the deadband nonlinearity employed did not induce unstable limit cycles, which implies the attenuation of these bending modes found in the continuous-time control design was maintained, and consequently, closed-loop stability was achieved by the PWM control. Finally, a Kalman filter was implemented to provide an estimate of the rigid-body states for control. The filter provided a good response for both the discrete-time and PWM-controlled systems. Although the modes were still excited by the control firings, this excitation was ignored by the control law, and the modes were allowed to damp naturally.

Acknowledgments

This work was supported in part by the U.S. Army Research Office under Grant DAAH04-94-G-0227 and the NASA Johnson Space Center under Grant NAG-9-746.

References

[1]Shieh, L. S., Decrocq, B. B., and Zhang, J. L., "Optimal Digital Redesign of Cascaded Analogue Controllers," *Optimal Control Applications and Methods*, Vol. 12, Nov. 1991, pp. 205–219.

[2]Shieh, L. S., Zhang, J. L., and Sunkel, J. W., "A New Approach to the Digital Redesign of Continuous-Time Controllers," *Control—Theory and Advanced Technology*, Vol. 8, No. 1, 1992, pp. 37–57.

[3]Tsai, J. S., Shieh, L. S., and Zhang, J. L., "An Improvement on the Digital Redesign Method Based on the Block-Pulse Function Approximation," *Circuits, Systems Signal Process*, Vol. 12, No. 1, 1993, pp. 37–49.

[4]Sears, N., "On-Orbit Flight Control Algorithm Description," Charles Stark Draper Lab., Rept. CSDL-R-881, Cambridge, MA, Jan. 1976.

[5]Wie, B., and Carroll, S., "Pulse Modulated Control Synthesis for a Flexible Spacecraft," Guidance, Navigation, and Control Invited Lecture Seminar, NASA Johnson Space Center, Houston, TX, Feb. 1990.

[6]Elgersma, M., Stein, G., Jackson, M., Matulenko, R., and Caldwell, B., "Space Station Attitude Control Using Reaction Control Jets," *Proceedings of the IEEE Conference on Decision and Control* (Tucson, AZ), Inst. of Electrical and Electronics Engineers, New York, 1992, pp. 632–638.

[7]Bernelli-Zazzera, F., and Mantegazza, P., "Pulse-Width Equivalent to Pulse-Amplitude Discrete Control of Linear Systems," *Journal of Guidance, Control, and Dynamics*, Vol. 15, No. 2, 1992, pp. 461–467.

[8]Shieh, L. S., Yates, R. E., Leonard, J. P., and Navarro, J. M., "A Geometric Series Approach to Modeling Discrete-Time State Equations from Continuous-Time State Equations," *International Journal Systems Science*, Vol. 10, No. 12, 1979, pp. 1415–1426.

[9]Shieh, L. S., Dib, H. M., and McInnis, B. C., "Linear Quadratic Regulators with Eigen Value Placement in a Vertical Strip," *IEEE Transactions on Automatic Control*, Vol. AC-31, No. 3, 1986, pp. 241–243.

[10]Andeen, R. E., "The Principle of Equivalent Area," *Proceedings of the AIEE Pacific General Meeting* (San Diego, CA), Vol. 79, American Inst. of Electrical Engineers, Applications and Industry, 1960, pp. 332–360.

[11]Kirk, D. E., *Optimal Control Theory*, Prentice-Hall, Englewood Cliffs, NJ, 1970, pp. 115, 116.

[12]Zimpfer, D., "A Digitally Redesigned Pulse-Width Modulated Spacecraft Control," M.S. Thesis, Dept. of Electrical Engineering, Univ. of Houston, Houston, TX, Aug. 1994.